ISBN: 978-3-95450-201-1 doi:10.18429/JACoW-IBIC2018-WEPC16

DESIGN AND RADIATION SIMULATION OF THE SCINTILLATING SCREEN DETECTOR FOR PROTON THERAPY FACILITY

P. Tian, Q.S. Chen, K.Tang, J.Q. Li, K.J. Fan†
State Key Laboratory of Advanced Electromagnetic Engineering and Technology,
Huazhong University of Science and Technology, Wuhan 430074, Hubei, China

Abstract

A proton therapy facility based on a superconducting cyclotron is under construction in Huazhong University of Science and Technology (HUST). In order to achieve precise treatment or dose distribution, the beam current would vary from 0.4 nA to 500 nA, in which case conventional non-intercepting instruments would fail due to their low sensitivity. So we propose to use a retractable scintillating screen to measure beam position and beam profile. In this paper, a comprehensive description of our new designed screen monitor is presented, including the choice of material of the screen, optical calibration and simulation of radiation protection. According to the off-line test, the resolution of the screen monitor can reach 0.13 mm/pixel.

INTRODUCTION

Huazhong University of Science and Technology (HUST) has planned to construct a proton therapy facility based on an isochronous superconducting cyclotron, from which 250 MeV proton beam is extracted. The layout of HUST proton therapy facility (HUST-PTF) is shown in Fig.1, with the basic specifications listed in Table 1.

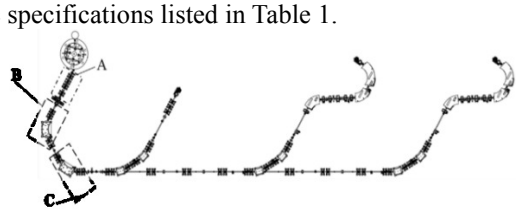

Figure 1: Layout of HUST proton therapy facility.

Table 1: Basic Beam Parameters of HUST-PTF

Phase	Energy/MeV	Current/nA
A	250	60-250
B	70-240	1-15
C	70-240	0.4-5

As the beam current is at the level of nanoampere, conventional non-intercepting instruments, such as inductive beam position monitors (BPMs), will fail to obtain effective beam signals without enough signal-to-noise ratio. Ionization chamber (IC) is popular for this kind of application, but it is too expensive to deploy IC all along the beamline. So we propose to use a relatively simple and economical instrument, scintillation screen, to measure beam position and profile.

The mechanical structure of the scintillation screen is shown in Fig.2. The CCD camera is located on the opposite side to the actuator, which is an air-driving type for the consideration of radiation damage.

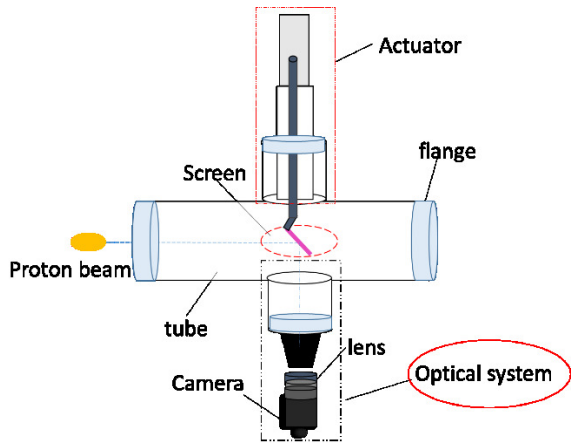

Figure 2: Scheme of retractable scintillator screen setup.

OPTIMIZATION OF SCREEN

Intercepting scintillation screens determine two-dimensional beam images and are frequently used for transverse profile measurements in beam transfer lines. High precision of profile and position measurements is important for controlling the spatial distribution of the beam [1]. For good luminescent screens, there are several key properties, including high efficiency of energy conversion, large dynamic range and good linearity between particles and light output, high radiation hardness and so on. Based on Refs. [2-4], the linearity of three common scintillators, separately YAG, P43, Al_2O_3:Cr are satisfied here when the current is 0.4nA. As for the photon yield related to energy deposition, P43 can produce higher number of photons. Figure 3 shows the different energy depositions of the three materials with thickness of 1 mm calculated by SRIM [5]. The luminescence intensity of the fluorescent screen with Al_2O_3:Cr was calculated by Eqs. (1) and (2) below

$$Y = \frac{\eta \times \Delta E \times n}{E_0} \quad (1)$$

with η the energy conversion efficiency, ΔE the energy loss of a particle，n the number of particles, E_0 the energy of the visible photon 3eV，thus yielding Y the number of the visible photons [6]. For particles of the beam, n is given by:

$$i = \frac{ne}{t} \quad (2)$$

with beam current i, e the charge of the proton, and t the width of the beam. Supposing the light output efficiency 0.2%, when beam current is 0.4 nA, the number of photon yield is 6.42×10^{11}/s, which is adequate for the CCD camera, with each pixel absorbing at least 1000-2000 photons [7].

* Work supported by national key R&D program, 2016YFC0105303.
† email address: kjfan@hust.edu.cn

ISBN: 978-3-95450-201-1 doi:10.18429/JACoW-IBIC2018-WEPC16

Because of the advantage of the higher ability of radiation hardness, the easier access and lower cost of the Al_2O_3:Cr than the other two materials, Al_2O_3:Cr has been given the priority in our design.

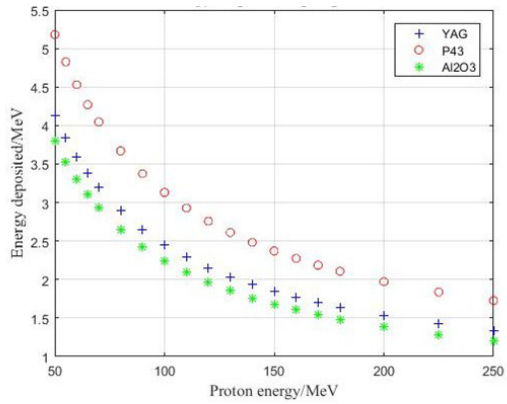

Figure 3: Fluorescent screen (1mm Al2O3:Cr, P43 and 1 mm YAG) with different beam energy).

As to the thickness of the screen, the resolution, heat production, scattering and other influences should be considered. The thinner the screen is, the better spatial resolution the setup will have. On the contrary, the light output will decrease. Referring to prior experiences [8, 9], the thickness of 1 mm was taken into account with the result of Bragg peak with 70MeV proton, shown in Fig. 4. The distance of 1 mm is far away from the Bragg peak, which is acceptable for the design.

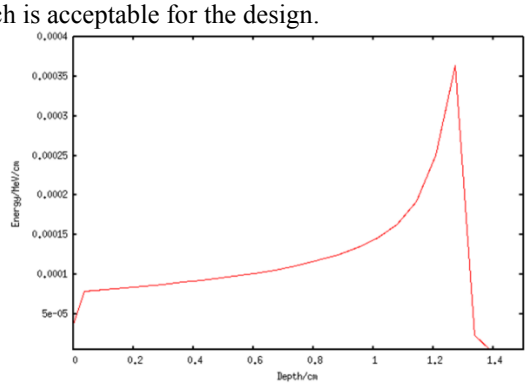

Figure 4: Bragg peak of Al_2O_3:Cr with 70MeV proton.

CALIBRATION

At present, the scintillating screen detector has been completed, with 1/2" CCD chip, 12-bit resolution, and monochrome, mounted with a distance of 200 mm with respect to the screen slightly below the optic axis. The camera was equipped with a Montex lens of 16 mm focal length. Figure 5 shows the off-line calibration field diagram of the setup. We used the five off-line pictures [one of them shown in Fig. 6(a)] to calculate the resolution and magnification, by using MATLAB to read and identify the pixel coordinates of the four vertices of square and cross, shown in Fig. 6(b). The number of pixels of each side (Table.2, Table.3) and the position of the central point of the cross are calculated, thus obtaining magnification, image resolution of the optical system and the accuracy of the repeated location. The two calibration results of square and cross can be used for cross validation.

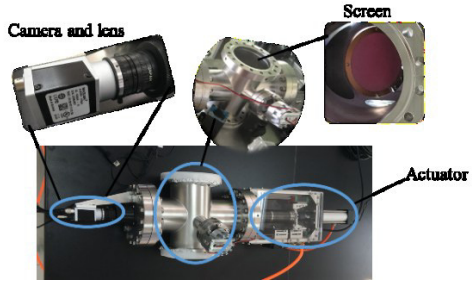

Figure 5: Off-line calibration of the setup.

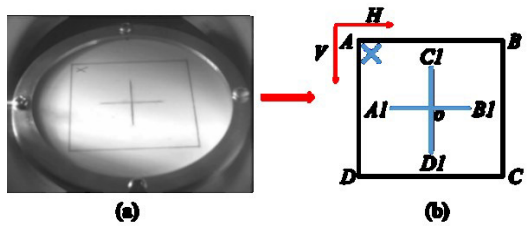

Figure 6: (a) One of the five off-line pictures; (b) Off-line calibration sketch map.

Table 2: Calibration in Square

Order	AB pixel	CD pixel	BC pixel	AD pixel
1	296	334	220	221
2	294	334	218	220
3	293	334	220	221
4	294	334	220	221
5	295	335	219	221
average	294.4	334.2	219.4	220.8
magnification	0.07771		0.07700	
resolution/(mm/pixel)			0.13	

Table 3: Calibration in Cross

Order	A1B1/pixel	C1D1/pixel
1	161	114
2	160	113
3	161	112
4	160	113
5	160	112
average	160.4	112.8
magnification	0.07953	0.07910
resolution/(mm/pixel)	0.13	

According to statistics, the repeated positioning accuracy and the resolution of the system induced from the data are respectively 0.0637mm and 0.13mm/pixel.

RADIATION CALCULATION

Semiconductor devices like CCD operating in a radiation field may undergo degradation due to total dose effect of ionization and displacement damage effect. The ionizing dose effects involve electron-hole pair production, and displacement damage effects coming from the nonionizing processes. Such degradation may cause the deformation of the image captured by CCD for the structure of metal-dielectric semiconductor will become

ISBN: 978-3-95450-201-1 doi:10.18429/JACoW-IBIC2018-WEPC16

sensitive to ionizing radiation [10, 11]. The dose and flux of the sensitive area are calculated using Monte Carlo software, FLUKA and Geant4 [12, 13], to estimate the radiation level the camera can accept. Figure 7 shows the model in FLUKA (same as in Geant4) and the calculated radiation field of the setup. The number of analog particles is 3×10^7.

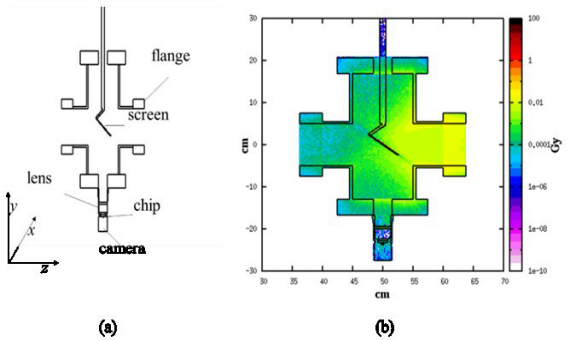

Figure 7: (a) The model in FLUKA; (b) Radiation field of the setup shown on y-z plane, the color band show the different level of dose distributed in the setup.

The dose of the chip simulated at 200 mm away from the screen is very low, on the order of 10^{-10}Gy. Under the condition of the energy 250 MeV and the current 500 nA, the cumulative absorbed dose is 154.65 Gy per year. While at the distance of 230 mm, the chip received a dose of 1.44 Gy per year, which is 0.5% of the tolerated dose. The dose absorbed by the chip at different locations from the screen varies from the distance, shown in Fig. 8, indicating that the smallest dose with distance of 230 mm.

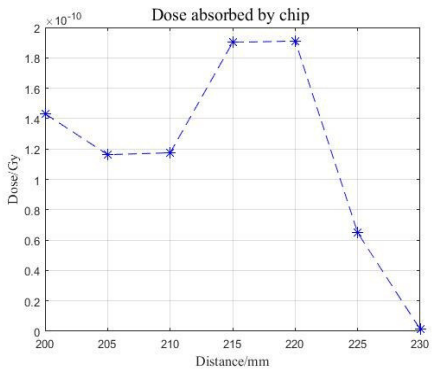

Figure 8: Dose in chip with different distance from screen.

Table 4: Flux Calculated from Geant4 and FLUKA

Flux(particles/cm^2)	GEANT4	FLUKA
proton	1.0269×10^5	4.6893×10^5
neutron	1.3041×10^7	1.8951×10^7

The flux of the two simulation software match well with each other (see Table.4), and both are lower than the tolerated range, respectively 10^{10} protons/cm^2 and 10^{12} neutrons/cm^2.

CONCLUSION

The intercepting method of scintillating screen has the advantages of simplicity and low cost, performing well in low beam current condition. The off-line calibration results of the optical system of the finished setup are fit for the measurement. The radiation dose absorbed by the chip within one year simulated by using FLUKA indicates that the camera needs periodic replacement within one year of operation. The number of particle fluxes through the chip simulated by FLUKA and Geant4 are very close, which reveals that the radiation level is relatively low. There is another choice of placing the camera at 230 mm to avoid more radiation, which will however enlarge the space, may be considered. As to the radiation shielding, various protective materials will be tested later to estimate the effects when using them.

REFERENCES

[1] A. Lieberwirth, W. Ensinger, P. Forck et al., "TEST OF THE IMAGING PROPERTIES OF INORGANIC SCINTILLATION SCREENS USING FAST AND SLOW EXTRACTED ION BEAMS," *in Proc. IBIC'16,* Barcelona, Spain, Sep. 2016, pp. 516-519, doi:10.18429/JACoW-IBIC2016-TUPG70

[2] Forck P, "Lecture Notes on Beam Instrumentation and Diagnostics," *JUAS, Darmstadt,* Germany, Jan. – Mar. 2011.

[3] Krishnakumar, Renuka, "Scintillation Screen Materials for Beam Profile Measurements of High Energy Ion Beams," Ph.D. thesis, Dept., Technische Universität, Darmstadt, 2016.

[4] A. Lieberwirth, W. Ensinger, P. Forck, and B. Walasek-Höhne, "Response of Scintillating Screen to Fast and Slow Extracted Ion Beams, *in Proc. IBIC'13,* Oxford, UK, Sep. 2013, paper TUPF21, PP. 553-554.

[5] SRIM, http://www.srim.org/.

[6] A. Eempicki, "The physics of inorganic scintillators," *J. Appl. Spec, vol. 62, No*. 4, 1995.

[7] M. Turner, B.Biskup, S.Burger et al, "The two-screen measurement setup to indirectly measure proton beam self-modulation in AWAKE", *J. Nuclear Instruments and Methods in Physics Research A*, 2017.

[8] B. K. Scheidt, "UPGRADE OF THE ESRF FLUORESCENT SCREEN MONITORS", *in Proc. DIPAC'03*, Mainz, Germany, May 2003, paper PM14, pp. 125-127.

[9] G. Kube, C. Behrens, "RESOLUTION STUDIES OF INORGANIC SCINTILLATION SCREENS FOR HIGH ENERGY AND HIGH BRILLIANCE ELECTRON BEAMS", *in Proc. DIPAC'10*, Kyoto, Japan, 2010, paper MOPD088, pp. 906-908.

[10] G. R. Hopkinson, J. Dale, and P. W. Marshall, "Proton Effects in Charge-Coupled Devices," *IEEE Trans. Nucl. Sci., vol.* 43, NO. 2, 614, 1996.

[11] S. Hutchins, M. Facchini, E. Tsoulou, "RADIATION TESTS ON SOLID STATE CAMERAS FOR INSTRUMENTATION," *in Proc. DIPAC'05*, Lyon, France 2005, paper CTWA02, PP.315-317.

[12] Andrew Welton, "Absorbed Dose and Dose Equivalent Calculations for Modeling Effective Dose", NASA Johnson Space Center; Houston, TX, United States, JSC-CN-21442, Jan 01, 2010.

[13] Geant4, http://geant4.slac.stanford.edu/.